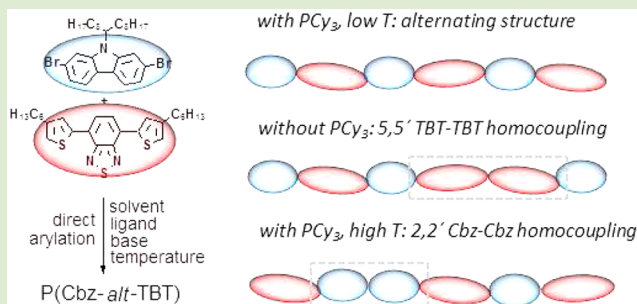


Identifying Homocouplings as Critical Side Reactions in Direct Arylation Polycondensation

Florian Lombeck,^{†,‡} Hartmut Komber,[§] Serge I. Gorelsky,^{||} and Michael Sommer^{*,†,⊥}[†]Makromolekulare Chemie, Universität Freiburg, Stefan-Meier-Straße 31, 79104 Freiburg, Germany[‡]Optoelectronics Group, Cavendish Laboratory, J J Thomson Avenue, Cambridge CB3 0HE, United Kingdom[§]Leibniz Institut für Polymerforschung Dresden e.V., Hohe Straße 6, 01069 Dresden, Germany^{||}Centre for Catalysis Research and Innovation and Department of Chemistry, University of Ottawa, Ontario, K1N 6N5, Canada[⊥]Freiburger Materialforschungszentrum, Stefan Meier-Straße 21, 79100 Freiburg, Germany

Supporting Information

ABSTRACT: Homocouplings are identified as major side reactions in direct arylation polycondensation (DAP) of 4,7-bis(4-hexyl-2-thienyl)-2,1,3-benzothiadiazole (TBT) and 2,7-dibromo-9-(1-octylnonyl)-9H-carbazole (CbzBr₂). Using size exclusion chromatography (SEC) and NMR spectroscopy, we demonstrate that both TBT and Cbz homocouplings occur at a considerable extent. TBT homocoupling preferentially occurs under phosphine-free conditions but can be suppressed in the presence of a phosphine ligand. Cbz homocoupling is temperature-dependent and more prevalent at higher temperatures. By contrast, evidence for chain branching as a result of unselective C–H arylation is not found for this monomer combination. These results emphasize that particular attention has to be paid to homocouplings in direct arylation polycondensations as a major source of main-chain defects, especially under phosphine-free conditions.



Direct arylation polycondensation (DAP) is emerging as a straightforward method to construct conjugated materials from simple building blocks for use in organic electronics.^{1–5} Compared to classic cross-coupling techniques used for polycondensation of conjugated monomers, DAP offers simpler, shorter and cheaper reaction schemes for both monomer and copolymer synthesis. The main advantage compared to, for example, Suzuki⁶ or Stille⁷ polycondensations, is that functional groups do not need to be installed, as the C–H bond can be directly activated. Additionally, less (toxic) waste is produced during polycondensation. Moreover, due to the absence of additional metals such as magnesium, tin, zinc or copper, DAP is capable to produce materials with higher purity.⁸ During the past few years, several groups have made significant progress in using DAP for the synthesis of conjugated polymers that exhibit molecular weights (MWs) and properties comparable or even enhanced compared to conventional cross-couplings.^{1–4} To this end, a considerable range of suitable C–H monomers has been used so far, with thiophenes,^{9–11} thienopyrrolidone,¹² thienothiazole,¹³ bithiophene,^{14–16} tetrafluorobenzene,^{17,18} pyrrole,¹⁹ and diketopyrrolo-pyrrole^{20,21} being among them. Monomers with a single type of C–H bond as functional group for polymerization preclude branching, while the situation is less clear in monomers with multiple C–H bonds. In thiophene-based monomers, H_α is most reactive,²² and the fact that highly

regioregular poly(3-hexylthiophene) can be made from 2-bromo-3-hexylthiophene implicitly entails selective α -arylation.⁹ However, several papers report that H_β reacts intentionally or unintentionally, leading to branched or cross-linked structures.^{14–16,23,24} Such side reactions are unacceptable and will lead to altered optical, structural and electronic properties. Additionally, polymer yields are lower as cross-linked materials are no longer soluble, which is sometimes taken as an indirect indicator for cross-linking.¹⁶ However, β -activation of thiophenes can even be exploited to create branched polymeric architectures using simple chemistry.²⁴ Next to issues associated with unselective C–H functionalization, termination and side reactions in DAP need to be identified and eliminated to produce defect-free materials with high MW. While side reactions such as homocoupling or dehalogenation are known from, for example, small molecule DA²⁵ or Suzuki polycondensation (SPC),^{26,27} little attention has been paid to inasmuch such processes lead to main chain defects and termination in conjugated polymers made by DAP.²⁸

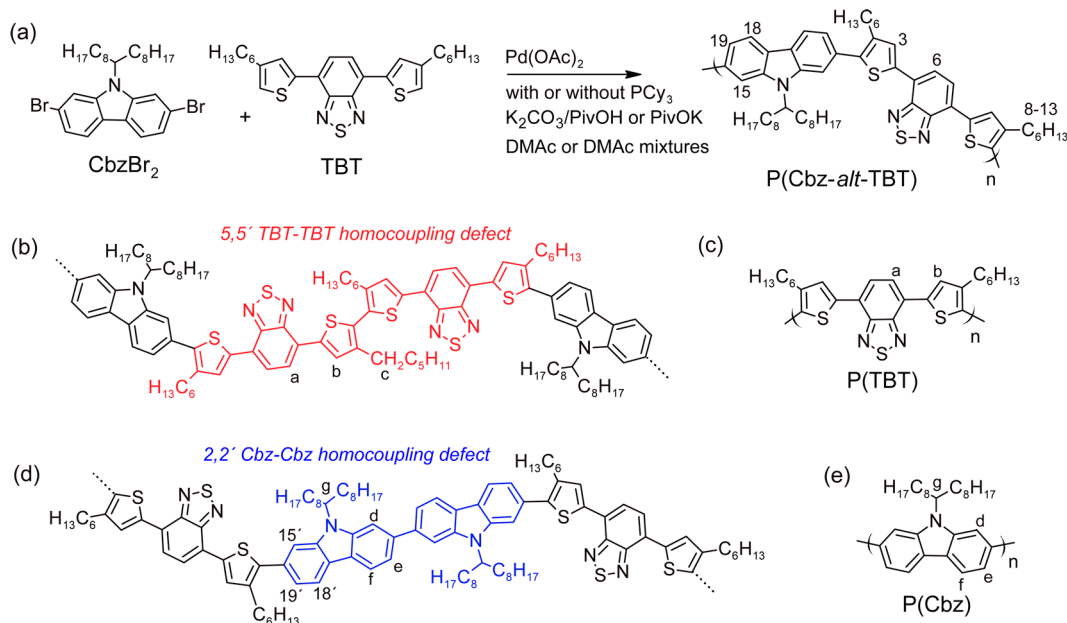
We investigated the DAP of 2,7-dibromo-9-(1-octylnonyl)-9H-carbazole (CbzBr₂) and 4,7-bis(4-hexyl-2-thienyl)-2,1,3-benzothiadiazole (TBT), particularly focusing on the extent

Received: July 8, 2014

Accepted: August 5, 2014

Published: August 7, 2014

Scheme 1. (a) Synthesis of P(Cbz-*alt*-TBT) via DAP, (b) Fragment of a P(Cbz-*alt*-TBT) Chain Exhibiting a 5,5' TBT-TBT Backbone Defect, (c) P(TBT) Homopolymer Made by Yamamoto Polycondensation, (d) Fragment of a P(Cbz-*alt*-TBT) Chain Exhibiting a 2,2' Cbz-Cbz Backbone Defect, and (e) P(Cbz) Homopolymer Made by Suzuki Polycondensation



of side reactions as a function of reaction conditions (Scheme 1a). The DAP of TBT and Cbz is particularly useful in several ways. First, both monomers exhibit three different C–H bonds, and hence, this system is well-suited to study possible branching and side.

Second, the resulting copolymer P(Cbz-*alt*-TBT), which is similar to the analog lacking hexyl side chains at the TBT unit (“PCDTBT”), is an interesting material for fullerene-based²⁹ or all-polymer photovoltaics.³⁰ Third, the two individual monomers are often copolymerized to give alternating copolymers with other monomers,^{31,32} which emphasizes the importance of understanding how these building blocks react under DAP conditions. Despite the large interest in DAP, the potential occurrence of side reactions has not been investigated in detail, and no generally applicable reaction parameters have emerged. Some common trends are visible though, including DMAc as a good solvent, tricyclohexylphosphine (PCy₃) as a good ligand, and a carboxylate as additive. Phosphine-free conditions, which are simpler and cheaper, are reported to proceed faster and to yield higher MWs.^{14,15,33–35} However, this trend is not always prevalent, as in some examples phosphine-free conditions did not improve MW.^{17,18} The parameters screened here included the choice of solvent, the presence or absence of PCy₃ as ligand, and the use of either potassium pivalate (PivOK) or pivalic acid (PivOH) in combination with K₂CO₃. A complete collection of all reactions performed is given in Table S1. The choice of an appropriate solvent was determined under the most simple conditions including Pd(OAc)₂, PivOK, and DMAc (entry 1).³⁴ Even though DMAc is not a particularly good solvent for most conjugated polymers, it is often used in DAP. The origin of this behavior is not fully understood, but it appears to be likely that DMAc fulfills certain functions within the catalytic cycle.²⁵ To balance solvency of P(Cbz-*alt*-TBT) and use of DMAc, 1:1 solvent mixtures with THF and toluene were considered in addition (entries 2 and 3). The resulting size exclusion chromatography (SEC) curves are shown in Figure 1a, and $M_{n,SEC}$ of 18.5, 24.0, and 6.5 kg/mol, and dispersities \bar{D} of 1.9,

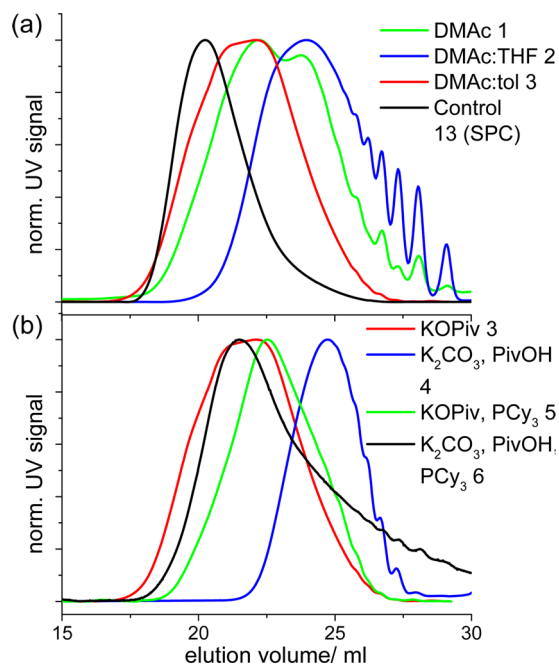


Figure 1. Size exclusion chromatography of P(Cbz-*alt*-TBT) via DAP in THF. (a) Influence of solvent (phosphine-free, PivOK, entries 1–3, 13) and (b) influence of the absence or presence of PCy₃ and base in DMAc/toluene (entries 3–6).

3.7, and 2.15 were obtained for DMAc, DMAc/toluene, and DMAc/THF, respectively, suggesting that DMAc/toluene was the best choice. Although polycondensation was fastest in pure DMAc, the MWs and yields were not reproducible arising from precipitates during polycondensation which did not redissolve. Therefore, the reaction time of entry 1 was shortened to 15 h to avoid precipitation, and all subsequent polymerizations were conducted in DMAc/toluene 1:1 mixtures, which gave the highest MWs and near quantitative yields of soluble products.

Surprisingly, the SEC curves in Figure 1a exhibited shoulders (DMAc/tol) or were bimodal (DMAc), which is unusual for a cleanly conducted polycondensation. The SEC curve of P(Cbz-*alt*-TBT) made by SPC with $M_{n,SEC} = 46.9$ kg/mol is shown for comparison (entry 13), exhibiting a monomodal distribution. Hence, one can assume that in P(Cbz-*alt*-TBT) made by DAP other processes next to the alternating coupling of CbzBr₂ and TBT monomers were present. To investigate this further, NMR analysis was carried out (Figure 2a–c). All spectra were

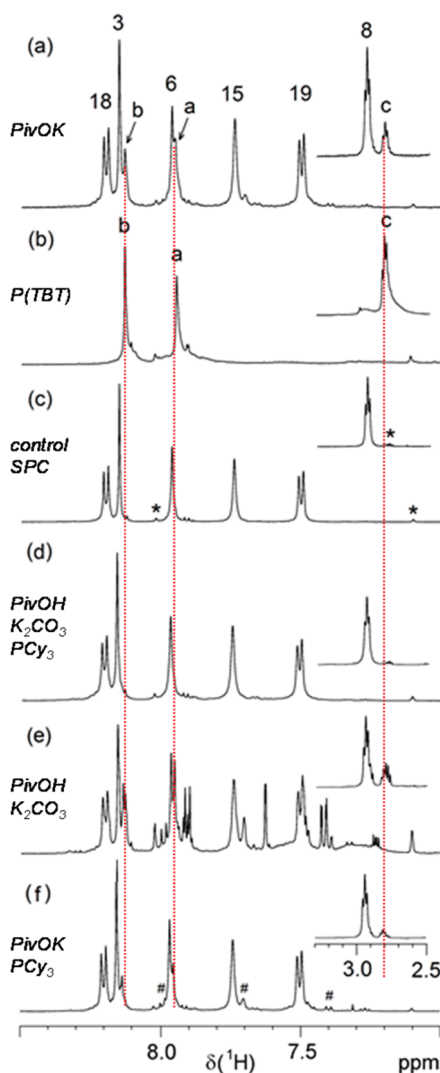


Figure 2. ¹H NMR spectra of P(Cbz-*alt*-TBT) in C₂D₂Cl₄ at 120 °C. (a) P(Cbz-*alt*-TBT) by DAP (entry 3), (b) P(TBT) by Yamamoto (entry 12), (c) P(Cbz-*alt*-TBT) by SPC (entry 13), (d) P(Cbz-*alt*-TBT) by DAP (entry 6), (e) P(Cbz-*alt*-TBT) by DAP (entry 4), and (f) P(Cbz-*alt*-TBT) by DAP (entry 5). Insets: region of methylene group next to thiophene. Signal numbering according to Scheme 1. #Cbz-Br end group; *thiophene-H end group.

recorded at 120 °C in C₂D₂Cl₄ to eliminate the effect of restricted rotation of the branched *N*-alkyl substituent, which results in signal splitting or line broadening at lower temperatures (Figures S1 and S2). On comparing the ¹H NMR spectra of entry 3 (Figure 2a) with that of P(Cbz-*alt*-TBT) made by SPC (entry 13, Figure 2c), additional signals at 8.13, 7.95, and 2.81 ppm (H_{a–c}) with considerable intensity become visible in the former.

Suspecting TBT homocoupling as the reason,³⁶ a TBT homopolymer was made by Yamamoto coupling (entry 12, Scheme 1c), whose main chain signals matched the additional ones of the spectrum of the P(Cbz-*alt*-TBT) sample of entry 3 (Figure 2b). Very indicative is the high-field shifted signal of the methylene group next to the thiophene ring (H_c). This proves that TBT homocoupling occurs in the DAP of P(Cbz-*alt*-TBT) under the conditions of entry 3 (Scheme 1b). Having identified this side reaction, we investigated its extent as a function of ligand (PCy₃ vs phosphine-free) and varying base (PivOK vs PivOH/K₂CO₃). The resulting SEC curves of entries 3–6 are shown in Figure 1b. Upon the addition of PCy₃, the very intense shoulder of entry 3 at the low elution volume side decreased but was still visible, possibly indicating reduced TBT homocouplings (entry 5). When the ligand was maintained and PivOK was replaced by PivOH/K₂CO₃, the SEC curve became monomodal, with some oligomeric intensity being still visible arising from moderate MW (entry 6). Interestingly, when PivOH/K₂CO₃ was maintained and the ligand was omitted, MW was drastically reduced in comparison to the first three cases (entry 4). In order to correlate the unusual shapes of the SEC curves, the samples were again subjected to ¹H NMR analysis (Figure 2a,d,e,f). From Figure 2a,d,e,f it becomes clear that in order to eliminate TBT homocoupling the presence of both PCy₃ and K₂CO₃/PivOH is needed. Both phosphine-free experiments (entries 3,4, Figure 2a,e) and that with PCy₃, but with PivOK instead of K₂CO₃/PivOH (entry 5, Figure 2f), did show the signals assigned to TBT homocoupling. The observation that PCy₃ as well as PivOH/K₂CO₃ was needed to suppress TBT homocoupling (Figure 2d) is highly interesting, as phosphine-free conditions are used in recent examples of DAP.^{14,34} It is therefore an interesting question inasmuch this side reaction is generic, or a specific feature of the monomer combination investigated here. From a mechanistic point of view, it seems obvious that the coordination sphere of palladium is one crucial factor that governs homocoupling, and that the use of bulky phosphines is required to suppress this side reaction. As acetate ligands are able to bridge two palladium centers, one plausible mechanism could involve the recombination of two equal chains with a terminal Pd complex, which could only be possible for sterically less demanding and bridging acetate ligands in the absence of phosphines.

We focused our interest not only on the additionally observed backbone signal arising from TBT homocoupling, but also on other low intensity signals. Figure S3 investigates the end groups of entry 8 with $M_{n,SEC} = 10.0$ kg/mol and $\bar{D} = 2.20$ by comparing the low intensity signals with the spectra of the monomers and the model compound CbzH₂. This comparison revealed the presence of H end groups both at the TBT and Cbz chain ends, while Cbz-Br end-caps were not detected in this sample. However, for P(Cbz-*alt*-TBT) made by DAP (entries 3–5) Br end-caps were observed (see Figures 2a,e,f and S4). The presence of Cbz-H instead of Cbz-Br chain ends importantly points to dehalogenation. This side reaction is known from small molecule DA, but its mechanistic origin remains unclear.²⁵ From the experiments presented here, it is not possible to draw reliable conclusions on the effects of reaction conditions on the extent of dehalogenation, and this will be a subject of future studies. Besides these end group signals, a set of three signals at 8.29, 7.75, and 7.63 ppm (H_{d–f}) appeared with varying intensities from sample to sample. Figure 3a shows an overlay of several spectra of P(Cbz-*alt*-TBT) made

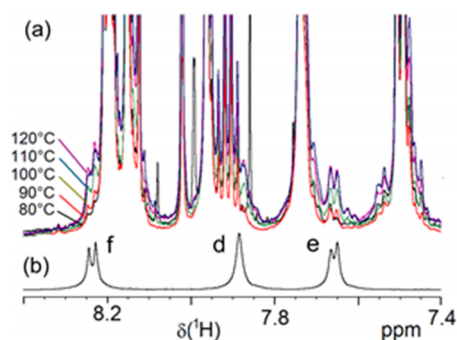


Figure 3. (a) Region of the ^1H NMR spectra of $\text{P}(\text{Cbz-}i\text{alt-TBT})_s$ synthesized at different temperatures (80–120 $^\circ\text{C}$, entries 7–11). (b) The same region of the ^1H NMR spectrum of $\text{P}(\text{Cbz})$. Signal numbering according to Scheme 1.

at different temperatures in the presence of PCy_3 and $\text{PivOH}/\text{K}_2\text{CO}_3$, conditions under which TBT homocoupling was absent (entries 7–11). The increasing intensities of these three signals with increasing temperature is clearly visible. ROESY and TOCSY spectra were crucial to unfold the nature of these new signals (Figures S5 and S6). While the TOCSY spectrum revealed that all three signals resulted from the same aromatic ring, the correlations between an additional NCHOct_2 proton signal at 4.75 ppm (H_g) and the two signals at 7.87 ppm (H_{15} , Scheme 1) and 7.75 ppm (H_d) observed in the ROESY spectrum suggested that the three new signals arose from an unsymmetrically substituted Cbz unit with only one side linked to TBT. Because there was no intensity correlation with end group signals rather than line broadening typical for backbone signals, a defect structure in the polymer was obvious. Suspecting Cbz-Cbz as a possible reason, we compared the signals with the spectrum of $\text{P}(\text{Cbz})$ made by SPC (entry 14, Scheme 1e, Figure 3b). This comparison confirmed protons d–f as the reason for these signals. The signals of the second half of the Cbz defect ($\text{H}_{15',18',19'}$) bonded to TBT have almost the same chemical shifts as those from the regularly alternating $\text{P}(\text{Cbz-}i\text{alt-TBT})$ structure and therefore overlap with backbone signals. These results clearly show that also homocoupling of two Cbz-Br chain ends is possible, and that low temperatures decrease the probability for this side reaction (Scheme 1d, Figure S7). Even at 90 $^\circ\text{C}$ the Cbz-Cbz homocoupling signal can be seen with very low intensity. The latter point is again highly interesting as many DAPs are carried out at elevated temperatures between 100 and 120 $^\circ\text{C}$ under similar conditions,^{1,3,4} pointing to possible halide monomer homocoupling reactions in other systems as well. Figure S8 compares the ^1H NMR spectra of entry 13 (SPC) with entry 6 (DAP) to better illustrate the content of Cbz-Cbz homocoupling in the samples with the best perfection of each method.

Next we turn back to our original motivation to investigate C–H selectivity in monomers with multiple C–H bonds for DAP. Chain branching is frequently discussed when using thiophene-based monomers having unblocked β -protons,^{14–16,23,28} but spectroscopic evidence is rare.²⁴ The Gibbs free energies ($\Delta G^\ddagger_{298\text{K}}$) of C–H bond cleavage of the α - and β -position in unsubstituted thiophene determined by density functional theory (DFT) for the concerted metalation-deprotonation (CMD) pathway are 25.6 and 29.9 kcal/mol, respectively.²² In view of this 4.3 kcal/mol difference in barriers for the α - and β -proton, unselective C–H arylation of thiophene-based monomers appears possible. While in the

TBT monomer used here the neighbored 4-position is blocked by the *n*-hexyl substituent, the 3-position is in principle available for unselective arylation. However, the detailed analyses of the proton NMR spectra of $\text{P}(\text{Cbz-}i\text{alt-TBT})$ suggested that unselective C–H functionalization of both the Cbz and TBT repeat units was not present with considerable intensity. Model reactions of TBT with an excess of pentafluorobromobenzene under the DAP conditions of entries 7–11 gave only mono- and disubstituted products (Scheme S1). DFT calculations were further performed in analogy with those for unsubstituted thiophene²² to estimate $\Delta G^\ddagger_{298\text{K}}$ of CMD cleavage for different C–H bonds in the TBT monomer. $\Delta G^\ddagger_{298\text{K}} = 25.4$ and 32.0 kcal/mol were obtained for the 5- and 3-positions, respectively (Scheme S2). Hence, the difference in the CMD barriers for C–H bond cleavage for the 5- and 3-protons increases from 4.3 kcal/mol in pristine thiophene to 6.6 kcal/mol in TBT. Whether the increased difference is caused by the *n*-hexyl chain or the electron-accepting benzothiadiazole group is not clear at present, but helps to explain that chain branching is experimentally not observed.

Finally, UV–vis spectroscopy was carried out to correlate homocoupling defects with optical properties. From Figure S9 minor differences can be seen, but these do not show consistent trends with increasing defect concentration. Apparently the similar absorption spectra of $\text{P}(\text{TBT})$ and $\text{P}(\text{Cbz-}i\text{alt-TBT})$ and possibly the presence of both TBT as well as Cbz homocoupling defects do not allow to establish defect-optical property relationships.

In conclusion, we have investigated the direct arylation polycondensation (DAP) of TBT and CbzBr_2 , focusing on side reactions such as chain termination, chain branching and homocoupling. Both TBT-TBT and Cbz-Cbz homocoupling can occur depending on the reaction conditions. By contrast, evidence for unselective C–H activation was not found. Using polymer yield and molar mass of polymeric products made by DAP as the only criteria for quality inspection is not sufficient and may hide important information on subtle details regarding backbone defects. Our results also suggest that the shape of a SEC curve can already be used as a simple indicator of homocoupling, which is experimentally more straightforward compared to high-temperature NMR measurements. Further studies that address mechanistic details and the question inasmuch these detrimental side reactions are generic features of DAP involving other monomers and catalytic systems are underway.

■ ASSOCIATED CONTENT

📄 Supporting Information

Materials, procedures, tables, additional NMR spectra and SEC curves, and details of DFT calculations. This material is available free of charge via the Internet at <http://pubs.acs.org>.

■ AUTHOR INFORMATION

Corresponding Author

*E-mail: michael.sommer@makro.uni-freiburg.de.

Funding

Financial support from the Fonds der Chemischen Industrie (FCI), the Research Innovation Fund of the University of Freiburg, the DFG (SPP1355), and the IRTG Soft Matter Science Graduate Program 1642 is greatly acknowledged. F.L. thanks the EPSRC for funding.

Notes

The authors declare no competing financial interest.

ACKNOWLEDGMENTS

The authors thank M. Hagios for GPC measurements and A. Hasenhindl for additional NMR measurements.

REFERENCES

- (1) Mercier, L. G.; Leclerc, M. *Acc. Chem. Res.* **2013**, *46*, 1597–1605.
- (2) Facchetti, A.; Vaccaro, L.; Marrocchi, A. *Angew. Chem., Int. Ed.* **2012**, *51*, 3520–3523.
- (3) Kowalski, S.; Allard, S.; Zilberberg, K.; Riedl, T.; Scherf, U. *Prog. Polym. Sci.* **2013**, *38*, 1805–1014.
- (4) Okamoto, K.; Zhang, J.; Housekeeper, J. B.; Marder, S. R.; Luscombe, C. K. *Macromolecules* **2013**, *46*, 8059–8078.
- (5) Wencel-Delord, J.; Glorius, F. *Nat. Chem.* **2013**, *5*, 369–375.
- (6) Sakamoto, J.; Rehahn, M.; Wegner, G.; Schlüter, A. D. *Macromol. Rapid Commun.* **2009**, *30*, 653–687.
- (7) Carsten, B.; He, F.; Son, H. J.; Xu, T.; Yu, L. *Chem. Rev.* **2011**, *111*, 1493–1528.
- (8) Estrada, L. A.; Deininger, J. J.; Kamenov, G. D.; Reynolds, J. R. *ACS Macro Lett.* **2013**, 869–873.
- (9) Wang, Q.; Takita, R.; Kikuzaki, Y.; Ozawa, F. *J. Am. Chem. Soc.* **2010**, *132*, 11420–11421.
- (10) Rudenko, A. E.; Wiley, C. A.; Tannaci, J. F.; Thompson, B. C. *J. Polym. Sci., Part A: Polym. Chem.* **2013**, *51*, 2660–2668.
- (11) Rudenko, A. E.; Khlyabich, P. P.; Thompson, B. C. *ACS Macro Lett.* **2014**, *3*, 387–392.
- (12) Berrouard, P.; Najari, A.; Pron, A.; Gendron, D.; Morin, P.-O.; Pouliot, J.-R.; Veilleux, J.; Leclerc, M. *Angew. Chem.* **2012**, *124*, 2110–2113.
- (13) Allard, N.; Najari, A.; Pouliot, J.-R.; Pron, A.; Grenier, F.; Leclerc, M. *Polym. Chem.* **2012**, *3*, 2875–2879.
- (14) Fujinami, Y.; Kuwabara, J.; Lu, W.; Hayashi, H.; Kanbara, T. *ACS Macro Lett.* **2012**, *1*, 67–70.
- (15) Kowalski, S.; Allard, S.; Scherf, U. *ACS Macro Lett.* **2012**, *1*, 465–468.
- (16) Mercier, L. G.; Aïch, B. R.; Najari, A.; Beaupré, S.; Berrouard, P.; Pron, A.; Robitaille, A.; Tao, Y.; Leclerc, M. *Polym. Chem.* **2013**, *4*, 5252–5260.
- (17) Lu, W.; Kuwabara, J.; Kanbara, T. *Macromolecules* **2011**, *44*, 1252–1255.
- (18) Wakioka, M.; Kitano, Y.; Ozawa, F. *Macromolecules* **2013**, *46*, 370–374.
- (19) Lu, W.; Kuwabara, J.; Kanbara, T. *Macromol. Rapid Commun.* **2013**, *34*, 1151–1156.
- (20) Guo, Q.; Dong, J.; Wan, D.; Wu, D.; You, J. *Macromol. Rapid Commun.* **2013**, *34*, 522–527.
- (21) Pouliot, J.-R.; Mercier, L. G.; Caron, S.; Leclerc, M. *Macromol. Chem. Phys.* **2013**, *214*, 453–457.
- (22) Gorelsky, S. I. *Coord. Chem. Rev.* **2013**, *257*, 153–164.
- (23) Rudenko, A. E.; Latif, A. A.; Thompson, B. C. *Nanotechnology* **2014**, *25*, 014005.
- (24) Okamoto, K.; Housekeeper, J. B.; Michael, F. E.; Luscombe, C. K. *Polym. Chem.* **2013**, *4*, 3499–3506.
- (25) Tan, Y.; Hartwig, J. F. *J. Am. Chem. Soc.* **2011**, *133*, 3308–3311.
- (26) Sommer, M.; Komber, H.; Huettner, S.; Mulherin, R.; Kohn, P.; Greenham, N. C.; Huck, W. T. S. *Macromolecules* **2012**, *45*, 4142–4151.
- (27) Jayakannan, M.; van Dongen, J. L. J.; Janssen, R. A. J. *Macromolecules* **2001**, *34*, 5386–5393.
- (28) Rudenko, A. E.; Thompson, B. C. *J. Polym. Sci., Part A: Polym. Chem.* **2014**, DOI: 10.1002/pola.27279.
- (29) Park, S. H.; Roy, A.; Beaupré, S.; Cho, S.; Coates, N.; Moon, J. S.; Moses, D.; Leclerc, M.; Lee, K.; Heeger, A. J. *Nat. Photonics* **2009**, *3*, 297–302.
- (30) Liu, X.; Huettner, S.; Rong, Z.; Sommer, M.; Friend, R. H. *Adv. Mater.* **2012**, *24*, 669–674.
- (31) Hou, Q.; Xu, Y.; Yang, W.; Yuan, M.; Peng, J.; Cao, Y. *J. Mater. Chem.* **2002**, *12*, 2887–2892.
- (32) Blouin, N.; Leclerc, M. *Acc. Chem. Res.* **2008**, *41*, 1110–1119.
- (33) Chang, S.-W.; Waters, H.; Kettle, J.; Kuo, Z.-R.; Li, C.-H.; Yu, C.-Y.; Horie, M. *Macromol. Rapid Commun.* **2012**, *33*, 1927–1932.
- (34) Choi, S. J.; Kuwabara, J.; Kanbara, T. *ACS Sustainable Chem. Eng.* **2013**, *1*, 878–882.
- (35) Lu, W.; Kuwabara, J.; Kanbara, T. *Polym. Chem.* **2012**, *3*, 3217–3219.
- (36) These were caused by asymmetrically substituted TBT units, hence, two explanations, branching at the TBT unit or TBT homocoupling were considered. The former was unlikely, as TBT branching should also lead to new carbazole signals with similar intensity, which were not observed.